Dynamical optical response of nematic liquid crystal cells through electrically driven Fréedericksz transition: influence of the nematic layer thickness References and links

Vittorio Maria Di Pietro, Aurélie Jullien, Umberto Bortolozzo, Nicolas Forget, Stefania Residori

Research Article | Vol. 26, No. 8 | 16 Apr 2018 | OPTICS EXPRESS 10716
Optics EXPRESS

Dynamical optical response of nematic liquid crystal cells through electrically driven Fréedericksz transition: influence of the nematic layer thickness

VITTORIO MARIA DI PIETRO,[1,2,*] AURÉLIE JULLIEN,[1] UMBERTO BORTOLOZZO,[1] NICOLAS FORGET,[2] AND STEFANIA RESIDORI[1]

[1] *Institut de Physique de Nice, Université de Nice Sophia-Antipolis, CNRS UMR 7010, 1361 route des Lucioles, 06560 Valbonne, France*
[2] *Fastlite, Les collines de Sophia, 1900 route des Cretes, 06560 Valbonne, France*
[*] *vittorio.dipietro@fastlite.com*

Abstract: A dynamical optical characterization of planar nematic liquid-crystal cells electrically driven through the Fréedericksz transition is presented. Our method involves applying voltage steps with different starting voltage close to the Fréedericksz threshold. Measurements are performed on cells with various thickness, from a few microns up to 180μm, and highlight the transient molecular disorder occurring close to the Fréedericksz transition. We show that the transient disorder affects the molecular arrangement mainly in the reorientational plane of the splay motion induced by the planar cell geometry. Moreover, a disorder quantification in terms of optical transmission losses and temporal dynamics enables us to picture the Fréedericksz transition. This characterization provides the identification of the electrical driving conditions for which the effect of the reorientational disorder is minimized. When comparing cells with various thicknesses, it results that thick cells are characterized by a much smoother transition with respect to the conventional step-like Fréedericksz transition of the thin cells, hence, thick cells can be dynamically driven over a large range of voltages, even below the Fréedericksz threshold. The results are discussed in view of novel electro-optical applications of thick layers of nematics. As an example, the experimental conditions for realizing a rapid birefringence scan and the achievement of a large and tunable group delay for femtosecond pulses are presented.

OCIS codes: (160.3710) Liquid crystals; (320.0320) Ultrafast optics.

References and links

1. C.-Y. Chen, C.-F. Hsieh, Y.-F. Lin, R.-P. Pan, and C.-L. Pan, "Magnetically tunable room-temperature 2π liquid crystal terahertz phase shifter," Opt. Express **12,** 2625–2630 (2004).
2. C.-S. Yang, T.-T. Tang, P.-H. Chen, R.-P. Pan, P. Yu, and C.-L. Pan, "Voltage-controlled liquid-crystal terahertz phase shifter with indium-tin-oxide nanowhiskers as transparent electrodes," Opt. Lett. **39,** 2511–2513 (2014).
3. A. Jullien, R. Pascal, U. Bortolozzo, N. Forget, and S. Residori, "High-resolution hyperspectral imaging with cascaded liquid crystal cells," Optica **4,** 400–405 (2017).
4. A. Hegyi, and J. Martini, "Hyperspectral imaging with a liquid crystal polarization interferometer," Opt. Express **23,** 28742–28754 (2015).
5. I. August, Y. Oiknine, M. AbuLeil, and A. Stern, "Miniature Compressive Ultra-spectral Imaging System Utilizing a Single Liquid Crystal Phase Retarder," Sci. Rep. **6,** 23524 (2016).
6. A. Jullien, U. Bortolozzo, S. Grabielle, J.-P. Huignard, N. Forget, and S. Residori, "Continuously tunable femtosecond delay-line based on liquid crystal cells," Opt. Express **24,** 14483–14493 (2016).
7. R. Laberdesque, A. Jullien, U. Bortolozzo, N. Forget, and S. Residori, "Tunable angular shearing interferometer based on wedged liquid crystal cells," App. Opt. **56,** 8656–8662 (2017).
8. S. Ge, P. Chen, Z. Shen, W. Sun, X. Wang, W. Hu, Y. Zhang, and Y. Lu, "Terahertz vortex beam generator based on a photopatterned large birefringence liquid crystal," Opt. Express **25,** 12349–12356 (2017).
9. C.-W. Chen, X. Guo, X. Ni, T.-H. Lin, and I. C. Khoo, "Slowing sub-picosecond laser pulses with 0.55mm-thick cholesteric liquid crystal," Opt. Mater. Express **7,** 2005–2011 (2017).
10. S.-T. Wu and D.-K. Yang, *Fundamentals of Liquid Crystal Devices* (John Wiley & Sons, 2006).

#319867 https://doi.org/10.1364/OE.26.010716
Journal © 2018 Received 23 Jan 2018; revised 7 Mar 2018; accepted 24 Mar 2018; published 12 Apr 2018

Optics EXPRESS

11. V. Freedericksz and V. Zolina, "Forces causing the orientation of an anisotropic liquid," Trans. Faraday Soc. **29,** 919–930 (1927).
12. G. I. Blake, T. Mullin, and S. J. Tavener, "The Freedericksz transition as a bifurcation problem," Dynamics and Stability of Systems **14,** 299–331 (1999).
13. P. G. De Gennes and J. Prost, *The Physics of Liquid Crystals* (Oxford Science Publications, 1993).
14. E. P. Raynes, C. V. Brown, and J. F. Stromer, "Method for the measurement of the K22 nematic elastic constant," Appl. Phys. Lett. **82,** 13–15 (2003).
15. H. Orihara, A. Sakai, and T. Nagaya, "Direct observation of the orientational fluctuations in a nematic liquid crystal with a high speed camera," Mol. Cryst. Liq. Cryst. **366,** 143 (2001).
16. M. Nespoulous, C. Blanc, and M. Nobili, "Orientational quenched disorder of a nematic liquid crystal," Phys. Rev. Lett. **48,** 0978010 (1993).
17. C. J. Gerritsma, C. Van Doorn, and P. Van Zanten, "Transient effects in electrically controlled light transmission of a twisted nematic layer," Phys. Lett. A **48,** 263–264 (1974).
18. G. Napoli, "Weak anchoring effects in electrically driven Freedericksz transition," J. Phys. A **39,** 11–31 (2006).
19. P. Manneville, "The transition to turbulence in nematic liquid crystals," Mol. Cryst. Liq. Cryst. **70,** 223–250 (1980).
20. M.G. Clerc, S. Residori, and C.S. Riera, "First-Order Fréedericksz Transition in the Presence of a Light Driven Feedback," Phys. Rev. E textbf63, 060701 (2001).
21. P. Tian, D. Bedrov, G. D. Smith, M. Glaser, and J. E. Maclennan, "A molecular-dynamics simulation study of the switching dynamics of a nematic liquid crystal under an applied electrical field," J. Ch. Phy. **117,** 9452–9459 (2002).
22. C. Vena, C. Versace,G. Strangi, S. D Elia, and R. Bartolino, "Light depolarization effects during the Freedericksz transition in nematic liquid crystals," Opt. Express **15,** 17063–17071 (2007).
23. F. Moss and P. V. E. McClintock, *Noise in Nonlinear Dynamical Systems, Volume 2 : Theory of Noise Induced Processes in Special Applications* (Cambridge University, 1989).
24. G. Agez, M. G. Clerc, E. Louvergneaux, and R. G. Rojas, "Bifurcations of emerging patterns in the presence of additive noise," Phys. Rev. E. **87,** 04291901 (2013)
25. I.-C. Khoo, *Liquid Crystals, Physical Properties and Nonlinear Optical Phenomena* (Wiley, 1995).
26. L. Lepetit, G. Chériaux, and M. Joffre, "Linear techniques of phase measurement by femtosecond spectral interferometry for applications in spectroscopy," J. Opt. Soc. Am. B **12,** 2467–2474 (1995).
27. J. Li, C.-H. Wen, S. Gauza, R. Lu, and S.-T. Wu, "Refractive Indices of Liquid Crystals for Display Applications," J. Display Techn. **1,** 51–61 (2005).

1. Introduction

Constantly growing applications of liquid crystals (LC) in photonics have recently been extended to novel electro-optical devices relying on their large birefringence. In this framework, electrically-addressed large cell gap nematics have attracted interests for terahertz phase shifters [1, 2], high-resolution hyperspectral imaging [3–5], phase and group delay control of ultrashort pulses trains [6], tunable angular shearing in wedge-shaped cells [7] and terahertz vortex beam generators [8]. In such progress, chiral nematics are not in rest with the recent demonstration of sub-picosecond pulse compression [9]. The common feature of these applications resides in the successful implementation and driving of thick LC-cells. For instance, LC layers ordered over more than 50 μm, until 200 μm for electrically-controlled planar nematics, have been shown to provide a large tunability of the optical properties of the LC-cells [3, 6]. However, the major drawback of thick LC-cell is the considerable increase of the relaxation and switching times. Emerging applications of thick LC-cells become more attractive as the cell response time decreases. Applying positive voltage steps is therefore more desirable relative to the passive relaxation that occurs after voltage switch-off, because the LC-cell response time scales with the inverse square of the applied voltage [10]. At this aim, the optical response and transmission have to be studied during the switch-on around the Fréederisckz transition (FT), in particular for thick nematic cells for which the response time limitations are more restrictive.

FT has been evidenced as early as 1927 [11] and can be pictured as a phase transition according to the bifurcation theory [12], providing a threshold voltage above which LC molecules start to reorient in order to minimize their free energy under the action of an externally applied electric field. We consider the situation where a nematic LC is confined between two substrates, with anchoring conditions determining the average orientation of the director, and undergoes the effects of an electric field applied between theses two substrates. Although the LC elasticity tends to maintain

Optics EXPRESS

the molecules along their initial direction, their dielectric anisotropy ($\Delta\epsilon = \epsilon_{\parallel} - \epsilon_{\perp}$) induces reorientation along the applied electric field (resp. orthogonally to the field), if $\Delta\epsilon > 0$ (resp. $\Delta\epsilon < 0$) in order to minimize their free energy. The competition between these two mechanisms results as a pitchfork bifurcation instability between two ordered patterns of molecules. The control parameter is the field strength and the threshold above which the molecules start to reorient is referred to as the Fréederisckz threshold voltage (V_{th}). Its value depends on the elastic constants, bend, twist and splay, characterizing the LC elastic deformations and on the dielectric anisotropy of the LC [13]. Several experimental methods to measure V_{th} of a given LC have been proposed. As a complement to capacitance measurement, optical methods are mainly based on transmission measurement between cross-polarizers, or the direct measurement of the phase shift due to the birefringence changes, or diffusion and optical scattering observation [14–16]. Besides, FT has been the subject of numerous theoretical and experimental papers, including twisted nematic cells [17], strong and weak anchoring conditions [18], turbulence around the phase transition [19], just to cite a few. The sub-critical character of the FT transition under the influence of a feedback field has also been studied [20].

In the framework of the above mentioned applications, molecular disorder and/or defect formation in LC-cells during the FT are of interest as they might induce significant optical losses. A microscopic model based on molecular-dynamics simulation of a nematic liquid crystal under the application of an electric field has been proposed [21]. There, it was shown that the order parameter $S(t)$ decreases monotonically when an electric field is applied. Reaching a minimum value S_{min} at time τ_{Smin} (corresponding to the maximum disorder), $S(t)$ presents an exponential recovery time that restores the nematic order. In a homeotropically aligned cell, a disordered switch-on dynamics has been confirmed through depolarization measurements during the application of a small voltage step around the Fréederisckz threshold voltage [22]. In this particular homeotropic configuration, a maximum depolarization related to the FT was attributed to disorder and defect formation at the reorientation onset. These studies are restricted to LC-cells with a thickness below 30 μm, and the scaling to larger nematic layers has not been studied so far. Moreover, no disorder has been evidenced for planar cells.

In this paper, we present an experimental study of the swich-on dynamics and disorder-induced losses during FT in planar nematic cells of different thickness. We highlight the different behaviors of thin versus thick cells and their possible impact on electrically-driven optical devices. Through the application of large voltage steps, we perform real-time optical measurements during the transient molecular rearrangement occurring at the switch-on. We show that during the onset of the FT the induced disorder occurs mainly in the extraordinary plane, that is, in the reorientational plane defined by the splay motion of the planar cell geometry. By quantifying the optical transmission on both polarization directions and its characteristic time-scale as a function of the cell thickness, we show that thick LC-cells are characterized by a much smoother transition with respect to the conventional step-like FT of the thin cells, hence, are less sensitive to the transient molecular disorder and can be dynamically driven over a large range of voltages, even below the Fréedericksz threshold. The performed measurements qualitatively agree with the predicted microscopic disorder [21], in addition, they enable us to dynamically picture the FT and to recover the transition voltage V_{th}. Finally, the analysis is extended to a fast measurement of the transient birefringence of a thick cell, reporting on the optimum electrical control for large group delay tuning of ultrashort optical pulses.

The experimental methods are described in section 2. The LC-cells are characterized by using two complementary setups, the first allowing dynamical measurements in the time domain, the second providing spectral maps in the frequency domain. The qualitative and quantitative influence of the initial conditions on the FT are investigated on the basis of the dynamical measurements performed with the first setup. The results are presented and discussed in sections 3 and 4. In section 5, the studies are extended by using the second setup to the measurement of

Optics EXPRESS

the transient birefringence when a thick nematic cell (L=180 μm fixed) is driven through the FT.

2. Experimental setup

The LC cells are made with a nematic LC mixture E7 inserted in between two $0.7mm$ thick fused-silica substrates. Both of them support a conductive layer of ITO (Indium-Tin-Oxide) as a transparent electrode. A thin film of polyvinyl alcohol (PVA) is spin-coated on the ITO layer and then rubbed with subsequent strong anchoring to align the molecules in a plane parallel to the substrate. All cells have a small pre-tilt ($< 1°$) in order to facilitate the director rotation in a single direction (one branch of the FT pitchfork bifurcation). Different thicknesses (L) of the cell gap, from 9μm to 180μm, are used with the same mixture of E7, for which $V_{th} \sim 1.2V$. We make a distinction between thick and thin cells for a cell gap above and, respectively, below 75μm. To study the dynamics of the electrically-induced FT, the LC-cells are connected to a waveform generator producing a sinusoidal AC voltage with variable amplitude, enabling the control of the average molecular orientation (θ). To prevent low-frequency electro-convection phenomena, the frequency of the electric field is fixed at 1kHz, so as to consider a quasi-static field for the LC molecules reorientation. The electrically-induced rotation of the nematic director leads to a variation of the refractive index of the extraordinary axis and, therefore, to a change of the LC-cell birefringence $\Delta n = n_e - n_o$, where n_e an n_o are, respectively, the extraordinary (parallel to the nematic director $\vec{n}$) and the ordinary (orthogonal to the nematic director $\vec{n}$) index of the nematic layer. The optical phase shift undergone by two cross-polarized components can, then, be written as $\Delta\phi = \frac{2\pi}{\lambda}\Delta nL$ with L the thickness of the birefringent medium.

We first focus on the polarization-dependent, disorder-induced optical losses during the FT. The experimental setup is shown in Fig. 1(a). A Helium-Neon laser emits a continuous radiation at λ=633 nm with 10 mW average power. A half-wave plate and a polarizer set the linear polarization direction at 45° with respect to the LC anchoring direction. This polarization alignment is done prior to any set of measurements and under a constant 10V bias voltage applied to the LC-cell. Then, the laser beam passes through a polarizing cube splitter that separates the two components of polarization, P (resp. S), parallel (resp. orthogonal) to the LC anchoring direction. Finally, each polarization component is recorded by a photodiode and the two respective signals are acquired by an oscilloscope.

The second experimental setup, shown in Fig. 1(b), allows the measurement of the phase shift undergone by a polychromatic pulsed light when passing through the LC-cell. The method relies on the broadband spectral interferometry technique with femtosecond pulses [26]. More details on the technique can be found in [3, 6]. A femtosecond laser, emitting pulses with a spectrum centered at 770 nm (120nm full width) and with 30 mW average power is sent through the LC-cell. A half-wave plate and a polarizer set the linear polarization direction at 45 ° with respect to the LC anchoring direction. A 180μm thick LC-cell have been used for these measurements. The principle is the following. When the pulse enters the cell, the components along the ordinary and extraordinary axis propagate with different group velocity, because of the refractive group index difference, and emerge from the cell as two sub-pulses delayed by $\Delta\tau_g = \Delta n_g \frac{L}{c}$, where Δn_g is the group index difference between the extraordinary, respectively, ordinary pulse and c is the speed of light in vacuum. When the cell is electrically driven, the molecular rotation on the extraordinary axis changes this delay. A second polarizer is placed at the exit of the LC-cell at 90 ° with respect to the first one. The resulting interference pattern is registered in the spectral domain where wavelength-dependent constructive and destructive interferences occur over the whole bandwidth. The interferogram is dynamically acquired by a OceanOptics spectrometer (2 ms integration time, 5 ms acquisition span , 0.3nm spectral resolution). The Fourier analysis of the fringed spectrum, then, enables us to recover the group delay $\Delta\tau_g$ (the harmonic position in the Fourier domain) and, thus, the group index difference Δn_g, with a precision only limited by the spectral resolution. Here, the precision on $\Delta\tau_g$ is ± 0.1fs, e.g. Δn_g is recovered with a

Optics EXPRESS

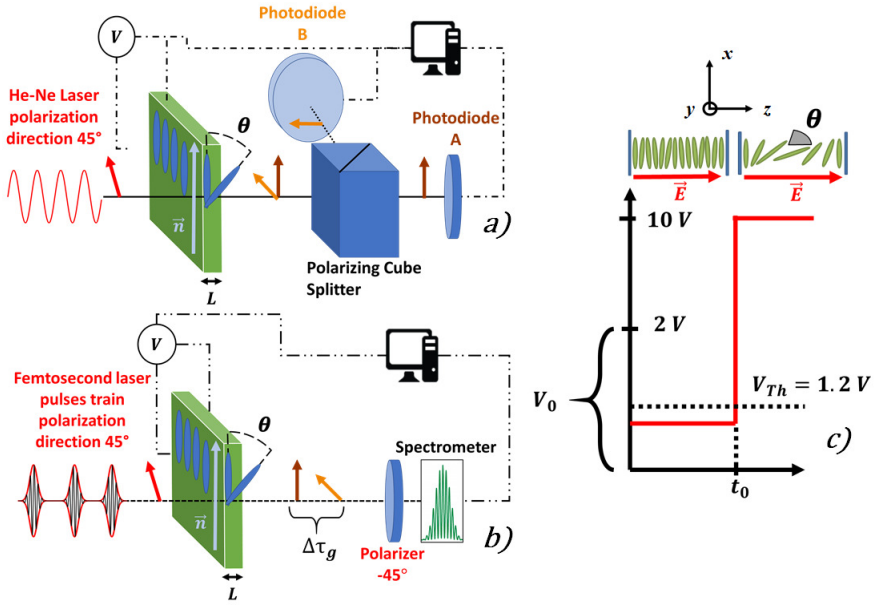

Fig. 1. Experimental setup for (a) the dynamical characterization of the FT and (b) the rapid birefringence scan. (a) A 10mW light beam from a Helium-Neon laser (λ = 633 nm) is sent onto the LC-cell after a half-wave plate and a polarizer that orientate its polarization direction at 45° with respect to the initial nematic director $\vec{n}$. The cube beam-splitter separates the two components of polarization at the output of the cell, each component is, then, sent to a photodiode. The photodiodes and the voltage generator are connected to the oscilloscope to acquire the polarization signals and a copy of the applied voltage. (b) A femtosecond laser (30 fs, repetition rate 80 MHz, spectrum centered at 770 nm) produces a 30mW beam. A half-wave plate and a polarizer orientate the input polarization at 45° with respect to the initial director of the LC-cell (L=180 μm fixed) to generate two cross-polarized sub-pulses delayed by $\Delta\tau_g = \Delta n_g \frac{L}{c}$ after the propagation in the LC. A polarizer placed at the output of the cell projects the two polarization components onto the same polarization direction in order to generate a spectral interference pattern. A spectrometer acquires the dynamical spectral map. In (c) is shown the voltage step applied to the LC-cells. V_0 varies from 0V to 2V, while the final voltage is fixed at 10V.

precision better than one part in a thousand ($1e^{-3}$, [6]). Furthermore, the method is resistant to laser amplitude fluctuations, as a moderate amplitude decrease of one sub-pulse will lower the harmonic amplitude without any change of its temporal position. This amplitude decrease of one sub-pulse can be as high as 50% without affecting the Fourier Transform. Consequently, the birefringence of the medium is recovered separately from the optical losses.

In order to characterize the FT, several steps of voltage are applied to the LC-cells in both setups, starting at $t = t_0$ as shown in Fig. 1(c). All the voltage steps have different starting voltage (V_0), with V_0 higher or lower than V_{th}, but the same final voltage (V_1 =10 V), so that we probe the influence of passing through the FT threshold for reaching the same final ordered state. To avoid any memory effects, we respect a rest time of about 4 minutes between any two successive measurements. Note that the two methods provide complementary characterizations and allow a description of the FT both in terms of dynamical measurements (time domain, setup of Fig. 1(a)) and of spectral maps (frequency domain, setup of Fig. 1(b)).

Optics EXPRESS

3. Dynamical characterization of the Fréedericksz transition

We first focus on the polarization-dependent dynamical behavior of the cells under the application of different voltage steps (setup of Fig. 1(a)) to LC-cells with various gap thicknesses. As an example, in Fig. 2(a) are plotted the signals acquired by photodiodes A and B during the cell switch-on for the two voltage steps given by $V_0 = 0V$ and $V_0 = 1.3V$ and for a $L = 14\mu$m-thick cell.

When V_0 is smaller than V_{th} ($V_0 = 0V$), a large optical transmission loss is detected on the extraordinary axis (photodiode A, blue lower curve) while no loss occurs on the ordinary axis (photodiode B, light blue upper curve). The sum of both signals is not constant over time, indicating an overall loss of transmission, rather that a simple energy exchange between polarizations. We explain this transmission decrease by optical scattering due to the induced molecular disorder. Indeed, as predicted in [21], the electrical switch-on of a LC-cell is associated with a reduction of the nematic order, following three stages : initiation, orientation and relaxation. This behavior is here qualitatively observed when $V_0 = 0V$. Consistently, the optical transmission losses are thus supposed to be induced by the molecular rearrangement, characterized by a strong disorder when passing through the FT. Losses are found mainly in the extraordinary plane selected by the splay motion of the planar cell geometry, indicating a minor contribution of the twist elastic constant to the transient molecular disorder.

Conversely, when V_0 is higher than V_{th} practically no losses are detected (photodiode A and B for the red, respectively, orange curve). Only a relative energy exchange between A and B as a result of the overall reorientation is observed. These observations show a clear disorder dependence on whether or not V_{th} is included in the voltage step. The projections on ordinary and extraordinary polarizations are slightly different before and after t_0 because the reorientational movement described by the average director angle tilt $\theta(t)$, is not perfectly confined on the xz plane (see Fig. 1(c)) .

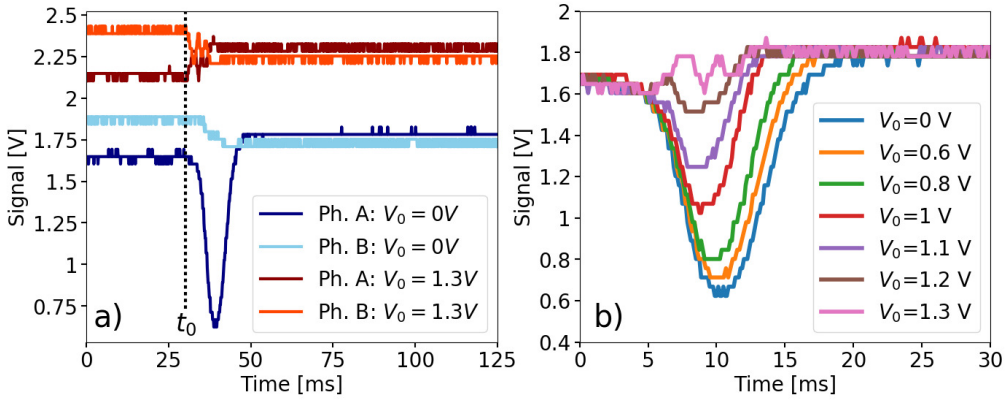

Fig. 2. a) Transmitted signals along the extraordinary (A, blue and red) and ordinary (B, light blue and orange) axis, acquired for a voltage step $V_0 = 0V - 10V$ and a voltage step $V_0 = 1.3V - 10V$ (L=14 μm). An artificial offset ($0.5V$) is added between the two sets of data for a better visibility. b) Transmitted signal from photodiode A (extraordinary axis) for the same cell (L=14 μm) and for different starting voltages V_0. All the measurements start from the same t_0 (not indicated in the plot for the sake of better visibility).

Figure 2(b) shows the signals measured by photodiode A (extraordinary axis) for the same cell (L=14 μm) and for different starting voltages, V_0 from 0 to 1.3V. All the measurements start from the same t_0 (not indicated in the plot). As it can be clearly appreciated from the different curves, increasing V_0 from $0V$ to $1.3V$ induces a progressive reduction of the disorder losses.

Optics EXPRESS

This set of measurements enables us to figure out a reduction of the order parameter when the LC-cell is driven through the FT, in a qualitative agreement with the predictions provided by the model simulations in [21].

When the starting voltage is above $V_{th} = 1.2V$, practically no losses are detected, and the molecular rearrangement occurs smoothly in this case. Furthermore, for the same applied voltage step ($V_0 = 0V$), a significant dependence on the LC thickness is observed. This is shown in Fig. 3(a), where the signal transmitted on the extraordinary axis and measured by photodiode A is plotted for a fixed voltage step ($V_0 = 0V$) and for different thicknesses of the LC-cell. The measurements show that thin cells present fast and huge losses (up to 60% for the thinner cells). Conversely, thicker cells exhibit lower maximum losses (higher minimum of the transmission dip), but these losses spread over a much longer time scale. Increasing the LC layer thickness, therefore, reduces the value of the maximum losses occurring close to the center of the transmission dip but also stretches the temporal scale for the complete switch-on to occur and over which the losses take place. These features are quantified in the following.

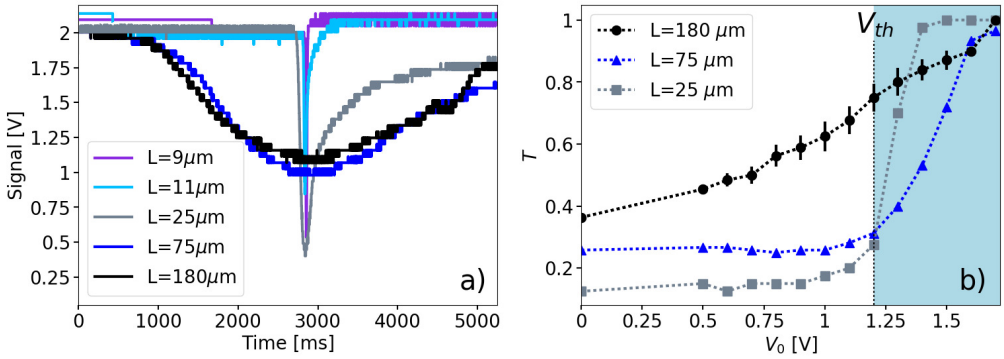

Fig. 3. a) Transmitted signal along the extraordinary axis (photodiode A) acquired during the cell switch-on for the same voltage step ($0V - 10V$) and for different LC thickness. Data are normalized and presented with an arbitrary temporal offset in order to compare the maximum losses (lowest value of the transmission dip). b) Transient transmission (see definition in the text) measured along the extraordinary axis during the cell switch-on for an applied voltage step V_0-10V by changing the starting voltage V_0 and for different cell thicknesses. The area beyond V_{th} ($1.2V$) is highlighted in blue.

In order to quantify the optical transmission losses, that mainly occurs along the extraordinary axis, we can define a transient transmission as follows: $T = \frac{I_{MIN}}{I_0}$, where I_{MIN} represents the minimum value reached by the signal A, thus, corresponding to the time of maximum disorder, and I_0 is its initial value. $T = 1$ means that no losses are detected on the extraordinary axis, i.e. the molecular arrangement occurs homogeneously. Instead, $T = 0$ represents a minimal transmission and, therefore, corresponds to the maximal disorder. The measured transient transmission evolution as a function of V_0 is plotted in Fig. 3(b) for some cells of different thicknesses (25, 75, 180 μm). The overall behavior of the transient transmission as a function of V_0 (Fig. 3 (a), is due to a balance between the thermal fluctuations and relaxation process. Hence, closer V_0 to the bifurcation point, greater the fluctuations, and the transient transmission.

The T value corresponding to the $0V - 10V$ step is changed accordingly to the cell thickness, as underlined in Fig. 3(a). Note that the 25μm cell has the most regular behavior, with a transmission as low as 0.1 when $V_0 < 1V$. Then, starting from $V_0 = 1.1V$, T increases rapidly up to 0.95 for $V_0 > 1.3V$. It is worth noting that the curve is a visualization of the FT, in compliance with

Optics EXPRESS

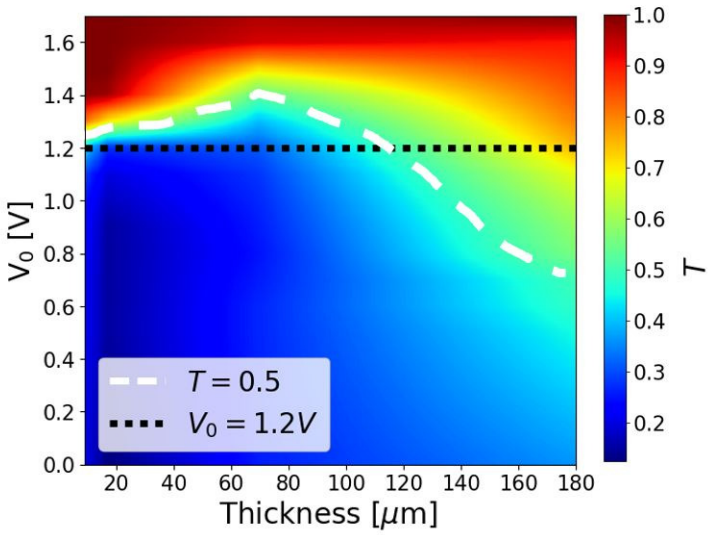

Fig. 4. Transient transmission (color-coded) as function of L and V_0, extrapolated from our experimental data. The dotted white line features $T = 50\%$.

the expected steep phase transition occurring at V_{th}. The proposed analysis thus represent an original dynamical method to evaluate the FT voltage threshold. However, the transition is largely spread out for the thickest cell (180μm). In that case, increasing V_0 also increases T, even for V_0 below the threshold. The 75μm cell has an intermediate behavior: an increase of T is noted for $V_0 = 1.1V$, but the slope is smoother than for the 25μm-thick cell. For the thickest cell of 180μm cell several identical measurements have been made (with the same V_0) in order to estimate the reproducibility. The data dispersion is also function of the FT: in particular when V_0 is smaller than $1V$ or greater than $1.4V$ the measurement is repeatable with a maximum uncertainty of 3%. Conversely when $0.9V < V_0 < 1.3V$ the error bar can reach a maximum of 9.5%. These fluctuations may be explained with the bifurcation theory: the statistical repartition of molecules in the two states of the pitchfork might change for successive measurements.

The above measurements demonstrate that the cell thickness affects the FT manifestation. Particularly, the transient molecular dynamics at the onset of the transition is characterized by optical losses on the extraordinary axis, which can be attributed to the microscopic spatial disorder, and whose features change when passing from thin to thick LC-cells. While thin cells present the expected step-like FT, with strong ($T \sim 0$) and localized in time molecular disorder, thick cells show a rounding of the transition, a phenomenon typically affecting bifurcations in the presence of noise (see, e.g., [23] and references therein, and [24] for a recent review). In our case, we can consider that the inner molecules of the cell are less affected by the anchoring strength than the molecules close to the cell surfaces, therefore, more affected by the disorder occurring at the transition point. Because several bifurcating modes are simultaneously excited and amplified by the transient disorder, we can expect this effect to be enhanced for thick cells, where the inner molecules experience more degrees of freedom to reorient, adding some noise to the bifurcation. Consequently, the transition rounding induces a larger molecular disorder when integrated over time, but simultaneously a lower maximum transient disorder around the threshold, because inner molecules tend to realign themselves more easily. Thus, when a voltage step is applied, although with V_0 below V_{th}, precursor modes with a non-zero projection along the extraordinary axis maintain the transient transmission value above 0. This realizes a pre-order state for which a

Optics EXPRESS

significative transmittance is obtained below V_{th}, even though the finally reoriented state is not reached yet.

These findings draw different types of applications for LC-cell switch-on, depending on the nematic layer thickness. Indeed, based on the measured data, obtained with cells with various thicknesses, an operating area of nematics as a function of their thickness and of the driving voltage can be proposed. This is illustrated in Fig. 4, featuring the transient transmission as a function of V_0 and L. According to this map, the optimum starting voltage for switch-on can be easily deduced from the tolerable losses for any cell thickness. Two noticeable features emerge out. On the one hand, for thin cells ($L = 20\mu$m or less), the transient transmission is maximum once V_{th} has been reached. On the other hand, thick cells ($L > 100\mu$m) can be driven well below the FT threshold with a transmission still above 50%. The transition between thin and thick cells can be located at 75 μm, when the slope of the 50% transmission is changed.

4. Temporal dynamical features

Another signature of the FT resides in the time scale of the dynamical optical transmission losses. In order to characterize the temporal dynamical features, we proceed as follows. We define τ_{min} as the temporal span between the launch of the electric field (t_0) and the moment of minimum transmission, e.g. the instant of maximum molecular disorder. In the same way, we define a precursor time τ_{prec} as the span between t_0 and the start of the decrease of the transmission, as illustrated in Fig. 5. τ_{prec} can be seen as the initiation of the FT.

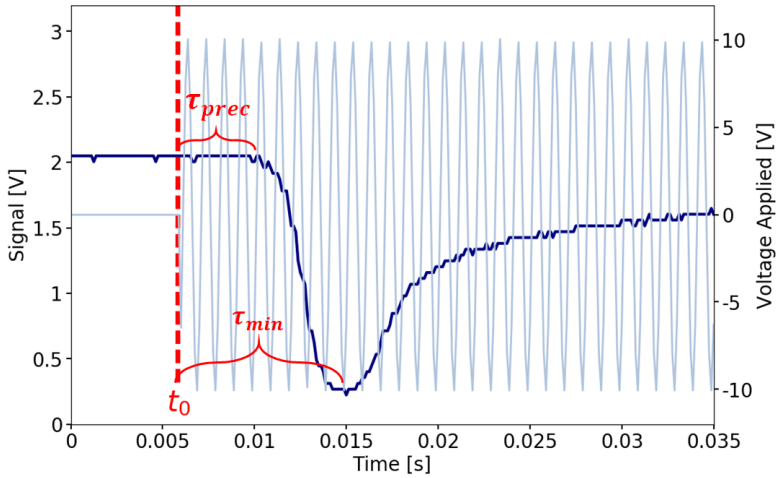

Fig. 5. Transmitted signal along the extraordinary axis from a L=9μm cell at $V_0 = 0V$ (blue line). Grey line represents the electric field applied. τ_{min} and τ_{prec} are indicated.

By following this procedure, we register τ_{min} and τ_{prec} as a function of V_0 for all cells (Fig. 6(a)- Fig. 6(c)). Both values are strongly affected by V_0 and by the cell thickness, and both exhibit similar trends. For thin cells, τ_{min} remains nearly constant with V_0 until $V_0 \sim V_{th}$, after which the temporal span for minimum transmission strongly decreases. We underline that this abrupt slope change is precisely localized to $V_0 = 1.2V = V_{th}$, establishing a dynamical measurement of the FT. This trend remains valid for all LC-cells, except the 180μm-thick cell, for which the shortening of τ_{min} starts for $V_0 > 0.5V$, well below the threshold. The curve then exhibits only a slight slope change over the threshold value. For very thick cells, as underlined in the previous section, the steepness of the phase transition is vanished. This is explained by the different strength imposed by the anchoring on the LC molecules, whether they are confined in a

Optics EXPRESS

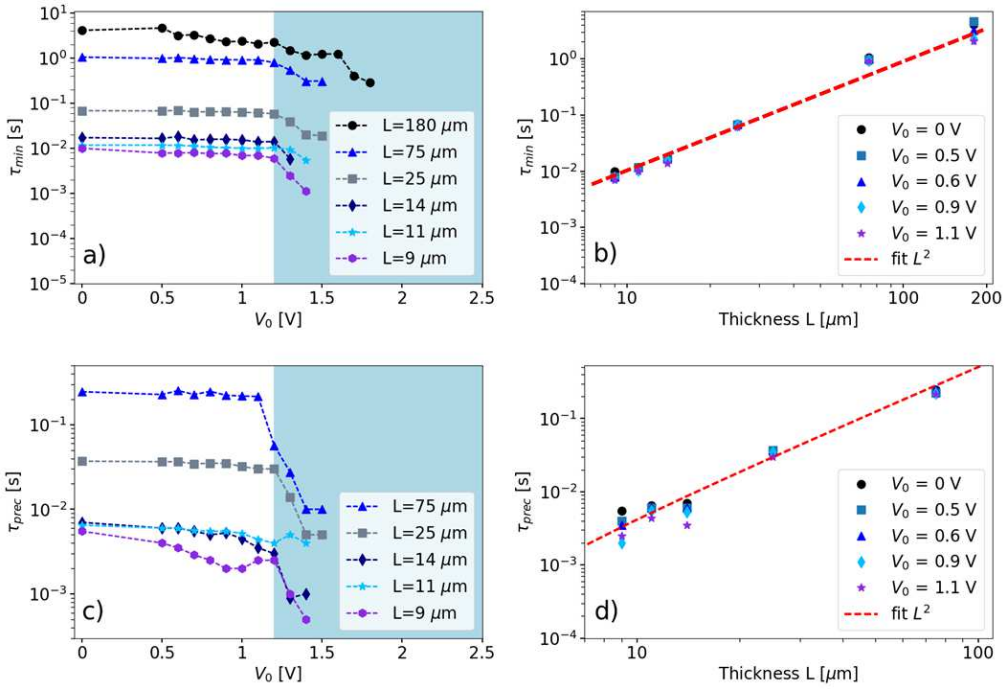

Fig. 6. Temporal dynamical features of the Fréedericksz transition. τ_{min} evolution as a function of V_0 and thickness (a, b), τ_{prec} as a function of V_0 and thickness (c, d). The area beyond the V_{th} (1.2V) is highlighted in blue (a,c) and the red line (b,d) indicates a quadratic fit of the data.

thin cell (in that case strong anchoring conditions dominate until V_{th}) or in a thick one (inner molecules undergo weaker anchoring constraints and reorient themselves faster).

Measuring τ_{prec} is less precise, especially for thick cells. Indeed, the measurement for the thickest cell was even not possible Fig. 6(c) . Nevertheless, the precursor time has the same qualitative behavior than τ_{min}.

The time scale of these values changes from hundreds of milliseconds to a few seconds, depending on the LC thickness. Fig. 6(b) (resp. Fig. 6(d)) shows τ_{min} (resp. τ_{prec}) as a function of the LC thickness for different values of V_0. Both the precursor delay and the time of maximal disorder depend quadratically on the thickness L of the nematic layer. Therefore, they both follow the characteristic switch-on time for LC displays [10, 25]. Our measurements indicate that the dynamical steps of the FT are all stretched with a quadratic dependence on L when increasing the LC-thickness. This is, furthermore, also an easy way to recover the V_{th} value.

5. Practical applications based on large birefringence in thick cells: rapid birefringence scan and large group delay tuning of ultrashort pulses

In this section, we illustrate the consequences of the FT transient transmission on the birefringence scan associated to the dynamical switch-on of a thick LC-cell. For the following measurements we have, thus, used the thickest, L=180 μm, cell.

The findings are of interest for new optical applications, such as the realization of tunable delay lines for ultrashort pulses or the implementation of LC based high-resolution hyperspectral imaging [3, 4, 6]. For these applications, a scan of the birefringent state is required with a large phase shift. Thus, thick LC-cells are needed. Additionnally, a rapid scan (a few seconds), such as

Optics EXPRESS

provided by a positive $V_0 - 10V$ voltage step, is desirable. At the lightning of our study of the dynamical FT and the results presented in the previous sections, V_0 has to be carefully determined in order to find the adequate balance between the FT-induced disorder losses and the reduction of the birefringence excursion due to a pre-ordered state ($V_0 > V_{th}$).

Conventional birefringence measurements usually rely on a monochromatic illumination of a LC-cell placed in between crossed-polarizers with its nematic director at 45° with respect to the polarizer axis. In that case, the transmitted intensity is written as $I_t = I/2(1 - cos(\Delta\phi))$ with $\Delta\phi = \frac{2\pi}{\lambda}\Delta nL$, where λ is the optical wavelength and Δn is the refractive index difference between the extraordinary and ordinary waves of the LC. This method allows to recover the intensity oscillations due to the reorientation induced phase shift between the two orthogonally polarized waves, however, it suffers from two drawbacks : the cosine dependence of the retrieved phase decreases the overall sensitivity and the measurement is affected by any change of the light intensity.

Here the measurement method relies on broadband spectral interferometry technique, as described in the experimental setup of Fig. 1(b). This method measures directly the group delay between two orthogonally polarized ultrashort pulses, thus, allows removing the uncertainties related to the light intensity fluctuations. A femtosecond laser pulse is divided into two orthogonally polarized sub-pulses, along the extraordinary, respectively, ordinary axis of the LC-cell. The two sub-pulses undergo a relative group delay $\Delta\tau_g = \Delta n_g \frac{L}{c}$ and, thus, produce an interference pattern when passing through a cross analyzer placed at the exit of the LC-cell. By analyzing the interferogram in the spectral domain, the group delay $\Delta\tau_g$ and, thus, the group index difference Δn_g, are recovered.

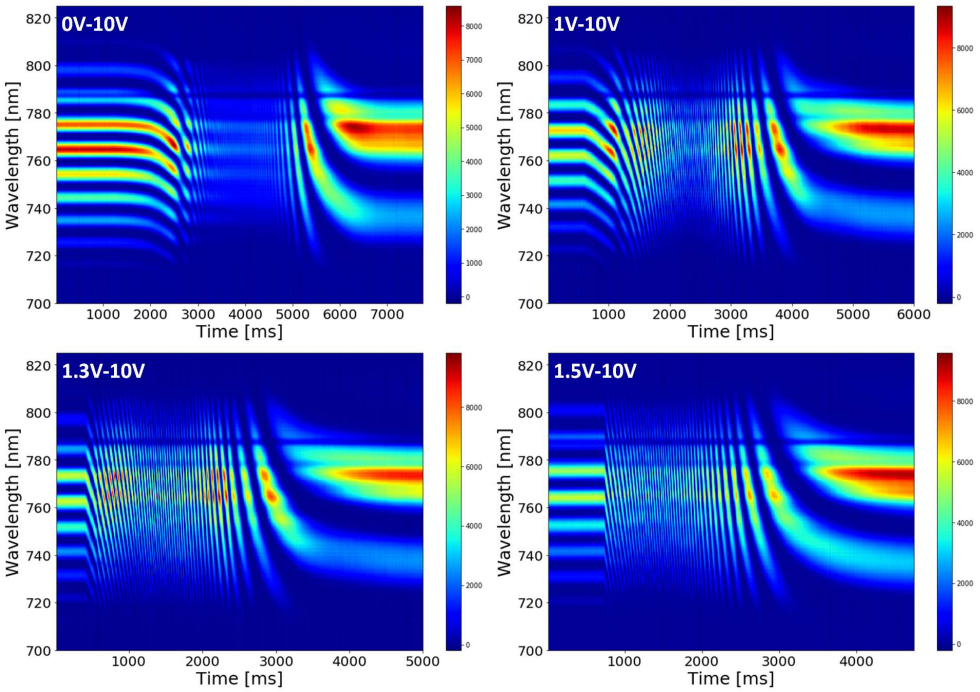

Fig. 7. Dynamical spectral maps obtained by using the experimental setup shown in Fig.1(b); data are acquired at $t = t_0$ for different V_0-10V voltage steps V_0=(0V-1V-1.3V-1.5V).

When no voltage is applied, the LC tilt angle $\theta = 0°$ and the birefringence is maximum, e.g. $\Delta n_g = \Delta n_{gmax} = 0.23$ for E7 [27]. Just as in the previous experiments, a $V_0 - 10V$ voltage step

Optics EXPRESS

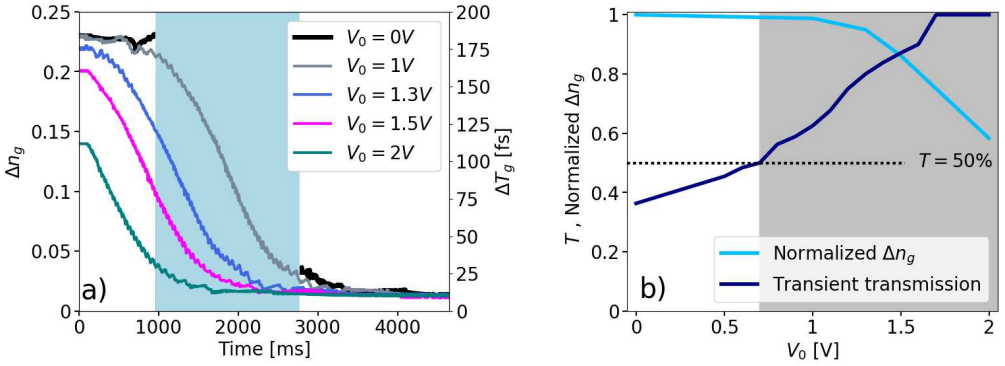

Fig. 8. a) Δn_g and $\Delta \tau_g$ plotted as a function of acquisition time for different V_0 $(0V, 1V, 1.3V, 1.5V)$; the blue area is associated to the $V_0 = 0$ measurement and indicates that for this voltage step the Fourier Transform is not possible in this time interval. b) Comparison between Δn_g normalized and the transient transmission T as a function of V_0 (the curve is extrapolated from the experimental data). In gray the condition of $T = 50\%$

is applied to the cell at $t = t_0$ $(V_0 = 0V, 1V, 1.3V, 1.5V)$. The spectral maps acquired during the dynamical switch-on following t_0 are shown in Fig. 7, while the retrieved temporal delay and birefringence as a function of acquisition time are displayed in Fig. 8(a).

When $V_0 = 0V$, the FT is clearly visible on the spectral map and the disorder losses on the signal are so strong that it is not possible to follow the trend of the interference fringes. As a consequence, the Fourier analysis is not possible in this case (highlighted blue zone in Fig. 8(a)). Only the initial and final Δn_g values can be measured, when the nematic order is restored. Conversely, when V_0 is $1V$, $1.3V$ and $1.5V$, the spectral fringes are distinctly visible, despite an overall loss of the fringes contrast. The temporal shortening of the transition is also visible. The birefringence dynamics is, then, correctly retrieved and all the measurements converge correctly towards the same value (0.053), i.e. Δn_g for $V = 10V$. These results are in accordance with our conclusions of section 3. For thick cells (180 μm in this case) the FT is not steep, but there is a gradual decrease in disorder losses when increasing V_0.

In particular, the $V_0 = 1V - 10V$ scan, although $V_0 < V_{th}$, provides a full birefringence excursion and an overall group delay tuning of $170fs$ in less than $4s$. According to Fig. 3(b), the transient transmission is not lower than 60% on the extraordinary axis, making this configuration admissible for several applications. It should be noted that the applied bias voltage $(V_0 = 1V < V_{th})$ enables to reduce the losses but not through a measurable pre-orientation of the inner molecules, as $\Delta n_g(t_0) = \Delta n_{gmax}$. This indicates a subtle change of the elasticity of the LC as a precursor state to the FT. Increasing V_0 naturally decreases the FT-induced losses, but the Δn_g excursion is decreased as well, as shown in Fig. 8(b). This figure features the normalized birefringence change and the transient transmission as a function of V_0 for the 180μm-thick cell. It can help to find out the compromise between the optical transmission losses and the overall birefringence scan for any application. This task can be satisfactorily accomplished, once a careful characterization of the LC cell has been performed and by appropriately choosing the optimal electrical driving conditions.

To summarize, thick LC-cells exhibit some different manifestations of the FT and, when appropriately driven, can be switched-on even below the FT threshold, making them good candidates for applications requiring a large birefringence scan, moderate losses and a commutation time of a few seconds.

Optics EXPRESS

6. Conclusion

To conclude, we have proposed an optical method to dynamically characterize the Fréedericksz transition through its induced transient molecular disorder. We found that this disorder occurs mainly on the reorientational plane of the splay motion and that it is strongly influenced by the cell thickness and by the applied starting voltage. We have quantified the optical transmission losses and the time-scale of the transition. While thin LC-cells present the expected steep and rapid transition near the threshold value ($V_0 \sim V_{th}$), it appears that for thicker cells the Fréedericksz transition is rounded, showing a gradual decrease in transient disorder losses when increasing V_0. The measurements enabled us to establish the optimum starting voltage for switch-on as a function of the cell thickness and tolerable losses. In addition, this approach is an original insight to picture the Fréedericksz transition and can even be used to measure the voltage threshold.

Furthermore, we have shown, that despite some optical transmission losses, thick LC-cells ($L = 180\mu m$) can be dynamically switched-on with a starting voltage slightly below the FT voltage threshold in order to get a full scan of the transient birefringent states and, therefore, exploiting the whole birefringence range that characterizes the nematic layer. These characterizations validate the use of thick LC cells for novel optical applications where the high birefringence of LC media can be efficiently exploited in thick layers by optimizing the electrical driving of the LC cell.

Finally, this study can be the framework of a general investigation on dynamics and defects formation in nematics around the FT. Experimentally, the driving electric-field frequency and of the LC-cell pre-tilt conditions [21] are expected to influence our observations. A theoretical description based on stochastic differential equations for the instability will also allow a deeper understanding of the presented phenomena.

Funding

Project Labcom SOFTLITE (ANR 15-LCV1-0002-01); European Union's HORIZON 2020 research and innovation programme under the Marie Sklodowska-Curie Grant Agreement (641272).